ELSEVIER

Journal of Structural Geology 28 (2006) 929–938

JOURNAL OF STRUCTURAL GEOLOGY

www.elsevier.com/locate/jsg

Geometric evolution of the Chelungpu fault, Taiwan: the mechanics of shallow frontal ramps and fault imbrication

R.V. Heermance [a,b,*], J.P. Evans [b]

[a] *Department of Geological Sciences, University of California, Santa Barbara, 1006 Webb Hall, Santa Barbara, CA 93106, USA*
[b] *Department of Geology, 4505 Old Mail Hill, Utah State University, Logan, UT 84322-4505, USA*

Received 20 August 2003; received in revised form 19 January 2006; accepted 25 January 2006
Available online 29 March 2006

Abstract

The September 21, 1999 $M_w = 7.6$ earthquake in Taiwan ruptured along the north–south-trending, east-dipping Chelungpu thrust fault that bounds the western foothills of the Taiwan fold-and-thrust belt. The near-surface (<4000 m deep) fault geometry changes from a simple wedge above a footwall ramp in the southern region, to a ramp–flat, bed-parallel geometry in the northern Chelungpu region. Rupture characteristics also varied between the northern and southern regions; higher frequency accelerations but lower velocity shaking was experienced in the southern region compared with the northern region. The hanging-wall flat, bed-parallel geometry of the northern Chelungpu region is the result of recent (~50 ka) fault migration ~1 km eastward away from the Sanyi fault trace. By contrast, the southern part of the Chelungpu fault is confined to its original trace that appears to have been active for much of the Quaternary. We show that this 'out-of-sequence' fault migration into the hanging wall in the northern region occurred due to the mechanics of the fault geometry at the leading edge of the thrust sheet where the shallow emergent thrust sheet is elongated due to the near-surface, bed-parallel flat. A simple mechanical model shows how resisting forces in the wedge-shaped hanging wall, which overrides a thick conglomerate sequence in the northern region, exceeds the tectonic load driving the slip of the thrust at the base of the wedge. In response, the fault forms a hinterland imbricate that shortens the hanging wall thrust sheet, reduces the volume of the emergent hanging-wall wedge, and thus reduces the resisting force. The southern region has a simple-wedge geometry that produces resisting forces in the hanging wall, to depths of 4000 m, that are less than or equal to the tectonic driving forces, allowing the thrust sheet to move without internal deformation or imbrication. This investigation of the Chelungpu fault indicates that hindward migration of an individual thrust fault can occur simultaneously with foreland-progression of the fold-and-thrust belt, given a shallow (<4000 m) footwall flat within the emergent thrust.

Keywords: Thrust faulting; Mechanics; Taiwan; Imbrication

1. Introduction

The Chelungpu fault ruptured in an $M_w = 7.6$ earthquake on September 21, 1999 (referred to as the ChiChi earthquake). The earthquake produced a 100-km-long rupture with vertical displacement up to 12 m (Y.H. Lee et al., 2001). The rupture displayed primarily thrust motion with oblique displacement at the northern and southern ends of the rupture (Lin et al., 2001; Lin et al., 2003). Though the 100-km-long rupture trace is continuous along the base of the foothills, where it separates the foothills from the Taichung basin to the west (Fig. 1), the fault structure and rupture characteristics varied significantly along strike. Investigation of the fault structure indicates a different geometry in the northern region than in the southern region of the fault (Fig. 2). The northern region ruptured along a steep, 45–60°, bed-parallel fault in the near surface to at least 250 m depth (Heermance et al., 2003). In contrast, the southern region ruptured along a 20–30°, east-dipping, footwall ramp where the fault cuts up-section (Tanaka et al., 2002; Wang et al., 2002a).

We investigate how the varying structure and geometry along the Chelungpu fault may have controlled the rupture style during the earthquake. The surface rupture from the ChiChi earthquake produced some of the largest displacements ever documented during a single earthquake (c.f. Wells and Coppersmith, 1994). The largest surface displacements were restricted to the northern region of the rupture approximately 40–50 km north of the epicenter (Y.G. Chen et al., 2001; Y.H. Lee et al., 2001; Lin et al., 2001). For this reason, we divided

* Corresponding author. Correspondence address: Department of Geological Sciences, University of California, Santa Barbara, 1006 Webb Hall, Santa Barbara, CA 93106, USA.
E-mail addresses: richard@crustal.ucsb.edu (R.V. Heermance), jpevans@cc.usu.edu (J.P. Evans).

0191-8141/$ - see front matter © 2006 Elsevier Ltd. All rights reserved.
doi:10.1016/j.jsg.2006.01.015

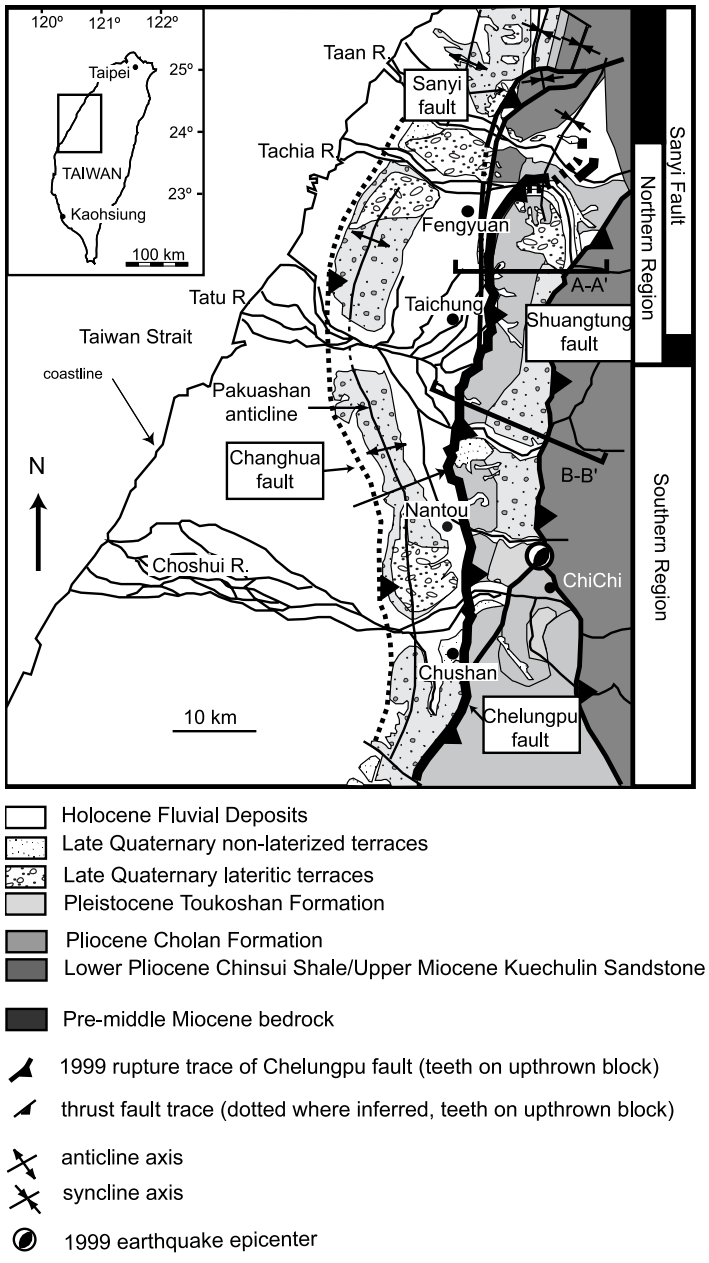

Fig. 1. Generalized geologic map of the Chelungpu/Sanyi fault region. Faults are shown as the bold black (9/21/99 earthquake trace) and thin black lines (dashed where inferred). Cross-sections A–A′ and B–B′ through the northern and southern regions are indicated. Map modified from Chang (1994), Chen et al. (2000), Ho and Chen (2000), and Lo et al. (1999).

the Chelungpu fault into the northern and southern regions (Fig. 1) based on surface displacement, the location of an eastward jog in the fault trace, and ground motion characteristics. Average vertical displacements were 4 m in the northern region, and reached a maximum of 12–15 m at the Shihkang Dam on the Tachia River (W.S. Chen et al., 2001; Y.G. Chen et al., 2001; Y.H. Lee et al., 2001). Horizontal displacements in the northern region averaged 8 m and reached a maximum of 11.1 m (W.S. Chen et al., 2001; Lin et al., 2001). Slip vectors in the northern region trend 320–330° based on surface rupture piercing points and GPS data indicating oblique thrust motion (W.S. Chen et al., 2001; Yu et al., 2001). In contrast, the southern region had only 2 m average vertical and horizontal displacements. Slip vectors trend 270–290° along a 20–30° dipping fault plane (Lee et al., 2001), indicating almost pure thrust movement in the central and southern parts of the ruptured fault.

Why the Chelungpu fault cut back into its hanging wall in one section of the fault, rather than maintaining slip on the Sanyi thrust, and how the varying fault geometry in the northern and southern regions affected the fault properties and rupture characteristics are investigated in this paper. We combine geologic map and cross-section analysis with results of the drilling through the fault tip (Tanaka et al., 2002; Heermance et al., 2003; Yue et al., 2005), and a simple mechanical analysis, to examine the conditions by which

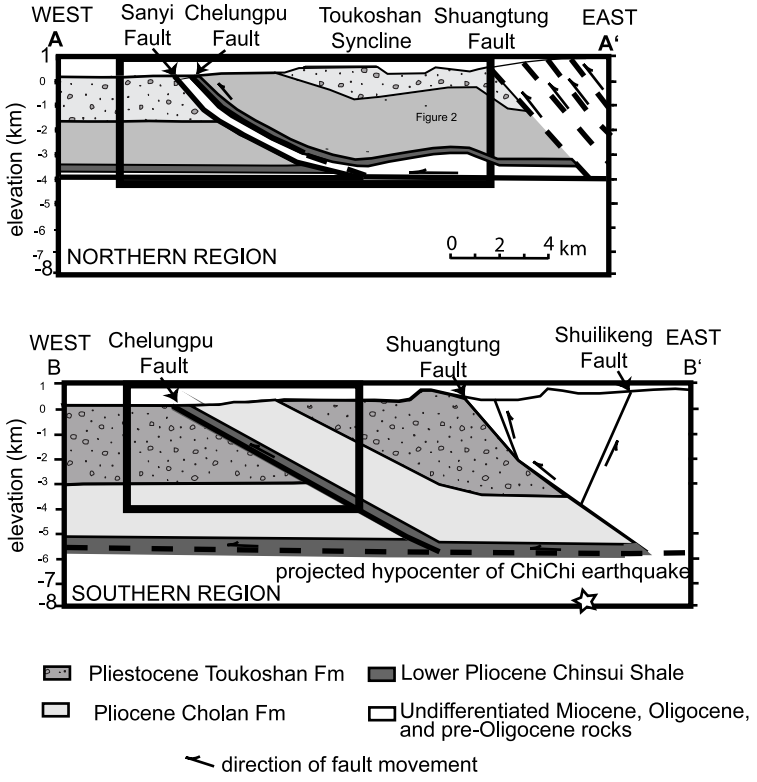

Fig. 2. Cross-sections through the northern and southern regions of the Chelungpu fault, modified after Yue et al. (2005). Faults are shown as bold black lines, dashed where approximated. The active rupture trace of the ChiChi earthquake is shown in the hanging wall of the Sanyi fault in the northern region. Cross-sections have the same scale and no vertical exaggeration. Boxed areas outline the fault structure to a depth of 4 km.

the thrust fault moves back into its hanging wall at the thrust tip at the northern region of the rupture.

2. Regional geology

The island of Taiwan has evolved due to structural thickening of sediments along the plate boundary between the Philippine Sea Plate and Eurasian Plate since the early Pliocene (Chi et al., 1981; Hsieh, 1990). Plate convergence is manifested in the southward propagating uplift of the mountains in Taiwan (Suppe, 1980, 1987). The Western Foothills geologic province is an active fold-and-thrust belt that runs along the western edge of the central mountains, and consists of Miocene through Quaternary sedimentary rocks accreted from the Eurasian margin (Ho, 1986; W.S. Chen et al., 2001), and deformed in a classic thin-skinned fold-and-thrust belt (Suppe, 1980).

The Chelungpu fault comprises the middle of three, north–south striking, west-vergent thrust faults in the Western Foothills geologic province (Fig. 1). The fault trace extends approximately 100 km NNE along the margin of the foothills (east) and the Taichung basin (west). The Shuangtung fault and blind Changhua fault roughly parallel the Chelungpu fault to the east and west, respectively (Fig. 1). These three faults make up the westward-propagating toe of the sub-aerial accretionary wedge created from oblique convergence of the Philippine Sea plate with the Eurasian continent (Davis et al., 1983; Ho, 1986). The southern region of the Chelungpu fault was probably continuous with another fault, the Sanyi thrust fault (Meng, 1963) to the north, during the early fault history, based on the continuous, north–south alignment of the faults and similar footwall deposits (Fig. 1). Both faults juxtapose Late Tertiary sediments with correlative Quaternary basin-fill along strike. However, this Sanyi/Chelungpu fault cuts up-section from the north to the south, because the Sanyi fault places middle Miocene units over thick Quaternary conglomerates (Hung and Wiltschko, 1993), the northern Chelungpu fault places Mio-Pliocene rocks over Quaternary deposits, and the southern Chelungpu fault places Pliocene Chinsui Shale over thin Quaternary conglomerate (Tanaka et al., 2002).

Timing of faulting in the Western Foothills fold-and-thrust belt is difficult to constrain precisely (Hung and Wiltschko, 1993). The Shuangtung and Chelungpu faults both cut the Pleistocene Toukoshan Formation, but the Shuangtung fault exhumes early and middle Miocene bedrock whereas the Chelungpu fault exhumes later Miocene and Pliocene bedrock in their hanging walls, respectively. The westernmost Changhua fault is blind but deforms Pleistocene deposits in its hanging wall. Though this evidence indicates all three faults were active during the Quaternary, in a general sense fault activity is probably progressing from the east to west, consistent with foreland propagation of the accretionary wedge (Davis et al., 1983). Paleomagnetic evidence suggests that deposition in the foreland basin increased at approximately 1.25 Ma (W.S. Chen et al., 2001) due to uplift in the proximal foothills, that is, slip on the Chelungpu and Shuangtung faults.

The Shaungtung thrust likely initiated during the early Quaternary around 1.25 Ma, followed by the Chelungpu fault between approximately 0.7 and 1 Ma, and ultimately by the Changhua thrust within the last 500 ka (Y.G. Chen et al., 2001; J.C. Lee et al., 2001; Mouthereau et al., 1999).

The Sanyi and southern Chelungpu regions have total displacements of at least 8 and 14 km, respectively (Hung and Wiltschko, 1993; J.C. Lee et al., 2001; Yue et al., 2005), and cut a thick (>1500 m) section of Quaternary Toukoshan Formation in the footwall. The northern region of the Chelungpu fault ruptured along a bed-parallel surface through late Miocene and early Pliocene bedrock at or near the surface, based on footwall outcrops near Fengyuan. The lack of any stratigraphic displacement across this northern region of the Chelungpu fault, combined with little to no syn-tectonic footwall deposits (Toukoshan Formation) and only ~300 m of slip (Yue et al., 2005) indicates that the northern region Chelungpu may be much younger than the Sanyi or southern Chelunpgu faults. The 1999 rupture also reveals that the Chelungpu fault is no longer continuous with the Sanyi fault, at least in the near surface, and that the Chelungpu fault northern region ruptured behind the Sanyi fault trace. The ~1 km map separation of these fault traces (Figs. 1 and 2a), combined with recent earthquake displacement on only the Chelungpu fault, suggests that contraction is accommodated along the northern Chelungpu fault in lieu of the 'older' Sanyi. The distinct fault traces indicate that strain has been localized along either the Sanyi or Chelungpu fault, as opposed to accommodated in a wide shear zone.

3. Fault structure

The northern region of the Chelungpu fault dips 45–60° east along a bed-parallel surface that follows late Miocene/early Pliocene bedding planes within 2–3 km of the earth's surface (Fig. 2a). This was determined by drilling through the fault at 250 m vertical depth (Tanaka et al., 2002; Heermance et al., 2003), field mapping, and seismic surveys (Wang et al., 2000, 2002b) across the fault. The hanging wall near the 1999 rupture trace consists of the Pliocene Cholan Formation, Pliocene Chinsui Shale (strike: 0–45°, dip: 35–70°E), and upper-Miocene Kueichulin Formations. Bedding becomes gentler (20–40°) eastward away from the fault trace towards the axis of the Toukashan syncline (Lo et al., 1999).

The northern region of the Chelungpu fault bends at ~3–4 km in the subsurface along a relatively flat detachment horizon in the Chinsui Shale. However, the Chinsui Shale is folded in the northern region into the Toukoshan syncline and the Tungshih anticline above a flat, lower detachment level in the Miocene Kuechulin Formation (Yue et al., 2005; Fig. 2). This lower detachment likely includes the Sanyi fault. Yue et al. (2005) suggest that slip is transferred from the Kuechulin detachment to the Chinsui Shale detachment via the Tungshih anticline. Alternatively, the fault could step up from the Kuechulin detachment into the Chinsui detachment.

The southern region of the Chelungpu fault shows a distinctly different structure from the northern region. Deep seismic reflection across the fault in the southern region (Wang et al., 2002a; Yue et al., 2005a) clearly reveals a planar fault geometry to 5–6 km depth (Fig. 2). The fault in the southern region dips 20–35° east in the near surface (Y.G. Chen et al., 2001; Tanaka et al., 2002) and cuts across relatively horizontal beds of Pleistocene and Pliocene stratigraphy in the footwall (Fig. 2b). Quaternary deposits of the Toukoshan Formation in the footwall are at least 1000 m thick in the southern region (Chang, 1971). The rupture does not follow pre-existing bedding planes in the footwall, at least in the near surface (<2 km).

4. Offset fluvial terraces

Offset fluvial terraces provide evidence for recent faulting and uplift along the northern part of the Chelungpu fault (Hsieh et al., 2001; Chen et al., 2002). Correlation of terraces across the fault provides strain markers that, given a terrace age, can allow the calculation of a minimum uplift rate across the fault. The Chelungpu fault contains multiple terrace levels in the hanging wall, but only one or two levels are preserved in the footwall (Hsieh et al., 2001; Fig. 3a). The terraces in the hanging wall are interpreted as abandoned fluvial surfaces exposed after tectonic uplift along the fault caused relative base-level to drop in the footwall, resulting in incision in the hanging wall (Hsieh et al., 2001).

The northern Chelungpu fault has fill terraces preserved 80–350 m above river level (Fig. 3a and b). These fill terraces consist of approximately 10 m of alluvium above an angular unconformity with the Cholan and Toukashan Formations (Hsieh et al., 2001) (Fig. 3b). Correlative terraces in the footwall of the Chelungpu fault are less than 30 m above river level. We interpret the fill terraces preserved in the hanging wall of the northern region to have formed at a time when the strath surface was near present-day river level, at the level of the correlative footwall terraces. Fill terraces require aggradation of the river channel above base level, and hence indicate that the hanging wall of the Chelungpu fault was a depositional environment for some time period, whereas it presently is being incised (eroded) due to recent uplift.

The southern region contains mainly strath terraces in the hanging-wall (Chen et al., 2002), without significant aggradation of alluvium above the strath. The terrace surfaces in the southern region of the Chelungpu fault do not correlate across the fault. These strath terraces likely formed during river incision through the hanging wall after a tectonically induced change in base level in the region, and hence did not form in the footwall.

The fill terraces in the northern region contain lateritic soil horizons interpreted to develop over long periods of time under tectonically stable conditions with intense weathering (Birkeland, 1999). Lateritic terraces in Taiwan are generally assumed to be older than 30,000 years. Lateritic terraces have been dated at 37,600–46,800 years old (Liu, 1990) from the northern part of Taiwan, near Taipei, 75 km north of the Chelungpu fault northern region. A general correlation may be made based on the lateritic soil development between the terraces in northern

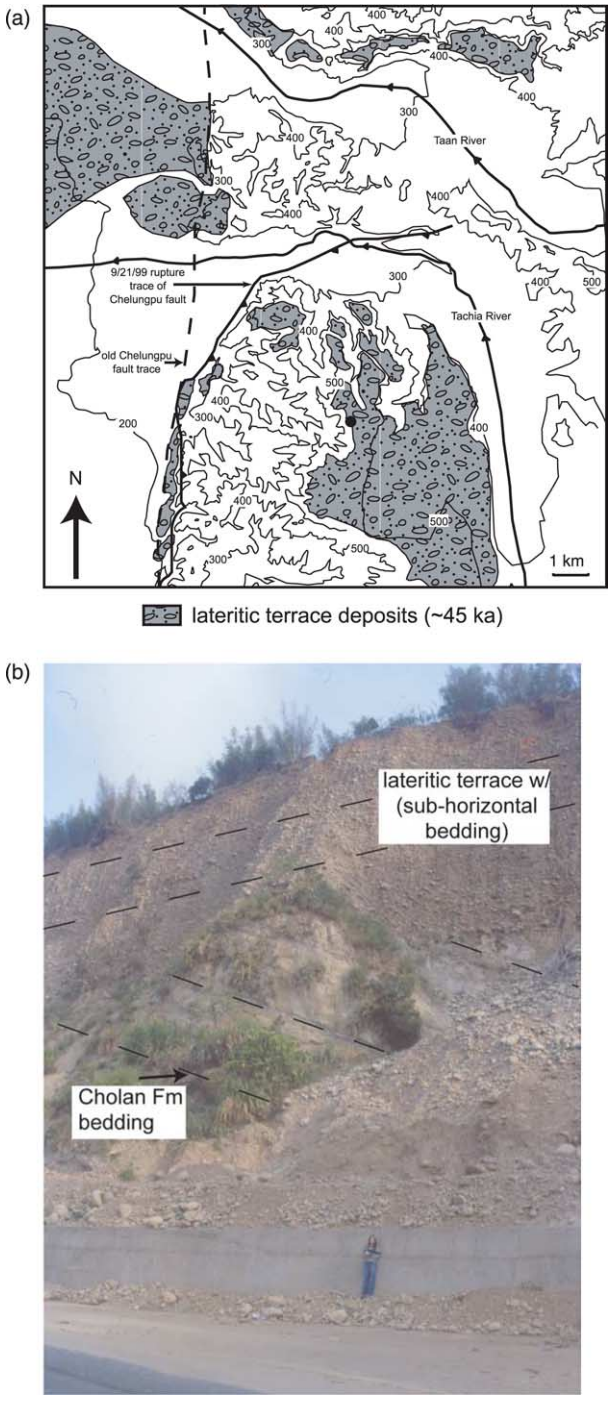

Fig. 3. Map (a) and photo (b) of lateritic terraces in the northern region of the Chelungpu fault. (a) Topographic map with 100 m contour lines (Chang, 1994; Lo et al., 1999; Ho and Lee, 2000; Ho and Chen, 2000). Fault traces are shown with teeth on upthrown side. Dotted lines depict major rivers flowing towards the west. Black dot in photo is location of photo in (b). (b) Photograph of uplifted lateritic terrace in hanging wall of the northern region of the Chelungpu fault. Person at base is 1.60 m tall. The terrace is a fill terrace ~10 m thick and 350 m above the adjacent river level. Bedding is depicted with the dashed lines. View is to the north.

Taiwan and the Chelungpu region. Climatic variation is minimal between these areas, and the topography is similar, indicating similar weathering processes are probably taking place in both regions. Therefore we suggest that the lateritic terraces observed in the Taichung region of Taiwan have ages similar to terraces observed near Taipei. The approximately 250 m vertical offset terrace elevation across the fault (Fig. 3a), divided by 45,000 years, yields an approximate uplift rate of 5.5 mm/yr. If we conservatively assume 3 m vertical offset during an earthquake, it would take one earthquake per 540 years to attain the observed offset. This seems reasonable for the active rates of tectonic processes in Taiwan. This uplift rate is also in good agreement with the ~1 cm/yr rock uplift rate determined from Holocene terraces in the southern Western Foothills thrust belt to the south of the present study area (Hsieh and Kneupfer, 2002).

We consider the effect of erosion on the thrust sheet, and specifically the effect of the Tachia River on the northern region. The Tachia River is one of the major drainages eroding the western slope of the Taiwan Central Mountain Range. The Tachia River flows west, but is diverted northward behind the hanging wall of the Chelungpu fault. The river again turns west where the Chelungpu fault bends east, and from there the river flows out to the Taiwan Strait. The hanging wall block that apparently 'diverts' the Tachia River is capped by lateritic fill terraces (Fig. 3a). Our hypothesis is that the Tachia River previously flowed due west, prior to uplift of the northern Chelungpu hanging wall but post-erosion of the Sanyi hanging wall, while depositing alluvium of the fill terraces. Movement on the Chelungpu thrust uplifted the hanging wall in the northern region causing northward diversion of the Tachia River east of the fault. Norris and Cooper (1997) noticed a similar geomorphic affect on the Waikukupa thrust in New Zealand, where the Wakukupa River effectively removed the hanging wall material, and this contributed to the formation of the 'out-of-sequence' imbricate thrust in the hanging wall. Faulting must have ceased for a period of time to allow fill terrace development and subsequent laterite formation in the northern region, and the cause of this paucity of activity will be discussed in the following section of this paper.

5. Mechanics of the thrust toe

One of the curious relationships shown by geologic mapping prior to the 1999 event, and the 1999 event itself, is that the active fault (northern Chelungpu thrust) lies approximately 1 km east of the Sanyi thrust trace (Fig. 1). We examine the mechanics of the shallow toe of the northern Chelungpu thrust sheet in order to determine why an emergent thrust, such as the Sanyi thrust, might form a hinterland imbricate. The simplest analysis considers a wedge of rock in two dimensions that is being driven by a tectonic load at the back part of the wedge. Resisting this force are the component of the weight of the wedge (acting parallel to the fault) and the resistant frictional force. This is essentially a restatement of the Hubbert and Rubey (1959) analysis, changed to consider a wedge-shaped block.

We evaluate the forces within the hanging wall that act to resist movement along a fault plane within 4000 m of the surface and use force equilibrium considerations to determine when the frontal wedge is stable, versus the point at which

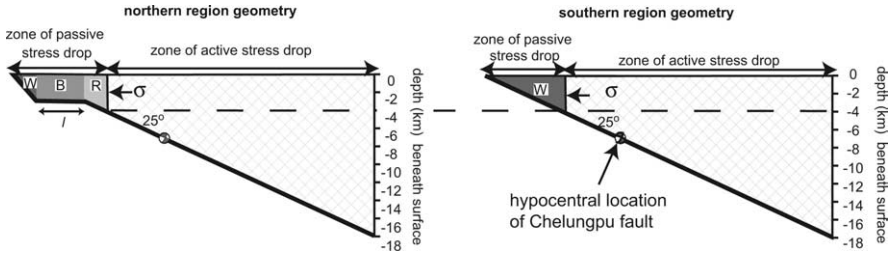

Fig. 4. Model parameters for the different geometries of the Chelungpu fault. The zones of 'passive stress drop' (solid gray) and 'active stress drop' (cross-hatched) are shown. Stress release during the earthquake produces a horizontal driving force (s) on the upper 4 km of hanging wall block. W, B, and R refer to respective parts of the hanging wall block that behave passively during earthquake rupture. Refer to text for description.

imbrication is favored. We use 4000 m as the cut-off depth where above this level the rock mass is moved passively relative to the lower regions of the fault (4–15 km) (Quin, 1990; Scholz, 1998). That is, the fault region above 4000 m does not store enough stress to produce energy during a fault rupture, and can be considered a 'passively' rupturing section of the fault. Movement within the upper 4000 m is therefore driven by displacement and energy release below 4000 m depth. Cohesion is not included in the analysis because cohesion values would offset each other in the passive and active regions of the fault.

The hanging wall of the Chelungpu fault from 4 km depth to the free surface can be viewed as an emergent thrust. A tectonic load drives this elongated wedge of rock from the back part of the wedge (Fig. 4a and b). The wedge consists of up to three parts, W, B, and R. Part W is the simple wedge at the front of the emergent thrust sheet (Fig. 4a). It is defined as an inverted right triangle with the top angle an approximation of the fault dip down to the level of the horizontal fault surface in the northern region (55°), and for the entire fault plane within 4000 m of the surface in the southern region (25°). Area B is the rectangular block of rock behind the frontal wedge. The block has length l that is defined as the distance along the footwall flat between the fault bends towards the hypocenter (Fig. 4a). For this analysis, l is assumed to be 6000 m, but will vary depending on the local fault geometry, which changes along strike (Heermance et al., 2003). The depth h is measured from the surface, assumed flat, to the subhorizontal fault between the fault detachments. Area R is the parallelogram-shaped area behind block B that accounts for the remaining volume of the hanging wall thrust sheet above 4000 m depth.

The forces in the horizontal, or x, direction resisting hanging-wall movement for the existing geometries in the northern and southern regions (Fig. 4) can be expressed in terms of the gravitational forces plus the frictional forces:

$$\text{N. Region resisting force} = w_{\mathrm{W}}\sin 55^\circ + w_{\mathrm{R}}\sin 25^\circ + \mu(w_{\mathrm{W}}\cos 55^\circ + w_{\mathrm{B}} + w_{\mathrm{R}}cos25^\circ) \quad (1)$$

$$\text{S. Region resisting force} = w_{\mathrm{W}}\sin 25^\circ + \mu w_{\mathrm{W}}\cos 25^\circ \quad (2)$$

where w = the weight (kg) of hanging wall areas W, B, and R = wedge, block, or rear block, respectively, and μ is the coefficient of friction. By incorporating rock density ρ (kg/m^3), gravitational acceleration (9.8 m/s^2), length (l) in meters for block B, depth h (m) to the base of block B, a coefficient of friction μ, a pore pressure term expressed as a ratio of the lithostatic load (Davis et al., 1983), and a total depth of the passive-rupture region of 4000 m, the total resisting force for the two areas in the wedge can be written as: Northern Region resisting force:

$$F_{\mathrm{r}} = \left[\frac{\rho g h^2}{2\tan 55^\circ}\right] + \sin 25^\circ\left[\frac{4000^2 - h^2}{2\tan 25^\circ}\right] + \cos 55^\circ \mu\left[\frac{\rho g h^2}{2\tan 55^\circ}\right] + \mu\rho g h l + \cos 25^\circ \mu\rho g\left[\frac{4000^2 - h^2}{2\tan 25^\circ}\right] \quad (3)$$

Southern Region resisting force:

$$\sin 25^\circ\left(\frac{\rho g(4000)^2}{2\tan 25^\circ}\right) + \cos 25^\circ\left(\frac{\rho g(4000)^2}{2\tan 25^\circ}\right)\mu \quad (4)$$

This expression is for the cohesionless dry state. If we consider the case of a thrust sheet with a fluid pressure (λ_{f}) in the fault zone (see Hubbert and Rubey, 1959; Willemin, 1984), the resisting force in the north becomes:

$$F_{\mathrm{r}} = \left[\frac{\rho g h^2}{2\tan 55^\circ}\right] + \sin 25^\circ\left[\frac{4000^2 - h^2}{2\tan 25^\circ}\right] + \cos 55^\circ \mu(1-\lambda_{\mathrm{f}})\left[\frac{\rho g h^2}{2\tan 55^\circ}\right] + \mu(1-\lambda_{\mathrm{f}})\rho g h l + \cos 25^\circ \mu(1-\lambda_{\mathrm{f}})\rho g\left[\frac{4000^2 - h^2}{2\tan 25^\circ}\right] \quad (5)$$

and the southern resisting force is given by:

$$\sin 25^\circ\left(\frac{\rho g(4000)^2}{2\tan 25^\circ}\right) + \cos 25^\circ\left(\frac{\rho g(4000)^2}{2\tan 25^\circ}\right)\mu(1-\lambda_{\mathrm{f}}) \quad (6)$$

where λ_{f} is the pore pressure as a ratio of the lithostatic load in the fault zone.

We examine the consequences of this force balance in Fig. 5. For a thrust wedge longer than 1 km, variations in h and l lead to changes in the resisting force on the wedge. As h increases, the force resisting motion at first increases to a

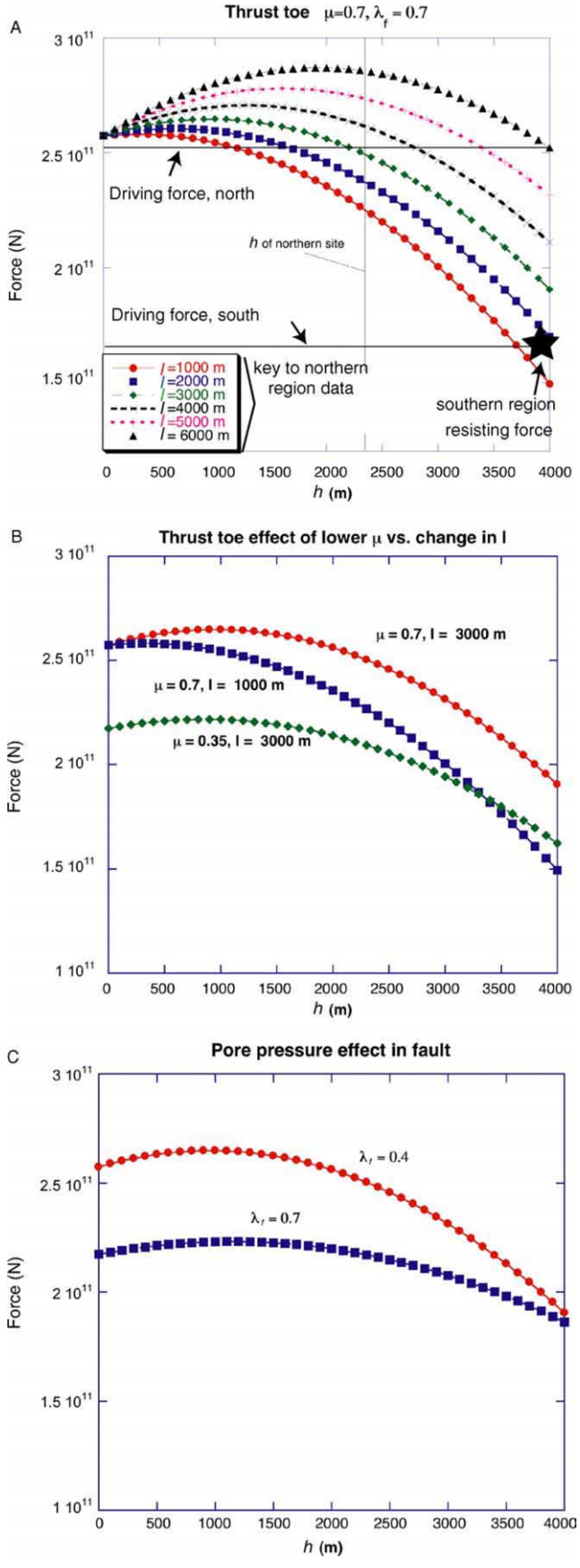

Fig. 5. Results of mechanical analyses for imbrication of the thrust toe. Force values are in newtons (N). μ=coefficient of friction. λf=pore pressure as a ratio of lithostatic load in the fault zone. (A) Plot of the resisting forces in the hanging-wall of the northern (convex-up graph lines) and southern (star) regions of the Chelungpu fault during the 9/21/99 earthquake as a function of the 'passive' hanging-wall thickness h, for different values of block length l. In the northern region, forces within the wedge initially increase with thickness h, and then decline. The value of h is interpreted to increase over time in the northern region due to deposition in the footwall and continued slip on the fault (Fig. 6). Thus, given the hanging-wall flat in the northern region, the resisting forces will increase in the hanging wall over time. This may force imbrication of the hanging-wall to maintain slip on the underlying footwall flat. In contrast, the resisting force in the hanging wall of the southern region does not vary due to the planar fault geometry, and this resistant force for the southern region is plotted as the star. The horizontal lines indicate the modeled driving forces calculated from the stress-drop during the 9/21/99 rupture for the northern and southern regions, respectively (Hwang et al., 2001). (B) Effects of changing the coefficient of friction and the length of the toe region. Reducing h decreases the driving forces needed to drive the toe, as does reducing the length, l. (C) Effects of pore fluid pressure on resistance to slip. Increased pore pressure reduces the force required to move the toe, which enables the toe region to be longer.

maximum, and then decreases (Fig. 5a). This is due to the increasing load applied to the back end of the wedge as h increases. As l increases, the resisting forces also increase due to the resistance to frictional slip in the fault zone. If the values of μ and γ are held constant, the mechanisms that can reduce the resistance to slip are either to decrease l or increase h. Decreasing the value of l can be accomplished by forming a hanging wall imbricate. An increase in h is also accomplished by hindward imbrication. Note that erosion in this case would reduce resistance up to the value of h_{max}, and then tend to increase the net resistance as h increases past h_{max}.

In the case of the northern part of the Chelungpu fault, where h=2300–2500 m and l is 5–6 km, the resisting force is near the maximum for that fault geometry (Fig. 5a) and is greater than the modeled driving force produced during the Chichi earthquake (Hwang et al., 2001). Thus, we suggest that the frontal toe is prone to hindward imbrication in order to reduce the resisting force in the hanging wall and therefore allow the toe to be moved forward.

An alternative means of reducing the resisting force is to reduce the coefficient of friction (Fig. 5b). Here, the resisting force is reduced along the thrust fault, and slip would tend to continue on the pre-existing fault. In the case of the Chelungpu fault, however, the frontal thrust rides over the conglomerates shed from the hanging wall. Heermance et al. (2003) suggest that the 1999 rupture occurred parallel to bedding in the shale-rich Chinsui Formation. Thus, we suggest that hindward imbrication is favored by the fact that frictional resistance to slip is likely to be greater where the thrust rides over conglomerates than where it juxtaposes shale on both sides.

Increasing the pore-fluid pressure decreases the resistance to slip (Fig. 5c; see Hubbert and Rubey, 1959). We saw little evidence for elevated pore fluid pressures in the uppermost portions of the fault (Heermance et al., 2003), but increased pore fluid pressures could be important at depths that have not been sampled by drilling.

The forces on the toe of the thrust along the planar fault in the southern region do not change within 4000 m of the surface (Fig. 5a), given that erosion keeps pace with uplift above the

ramp. Therefore, the rupture does not form a hinterland imbricate because of the planar fault geometry.

Increased volume in the hanging wall increases the magnitude of the resisting forces. For the existing conditions in the northern region, our model shows that resisting forces for the Sanyi fault would have been greater than the likely dynamic force produced during the 9/21/99 earthquake. Driving forces from the earthquake are calculated from the dynamic stress-drop and the fault area below 4000 m (Hwang et al., 2001) and are plotted in Fig. 5 as "driving force, south". This force is then converted to the horizontal direction. For existing conditions above the Sanyi fault (northern region) the wedge would not rupture given the driving forces produced during the 9/21/99 earthquake (Figs. 5a and 6). By breaking back into its hanging wall along bedding planes, the wedge effectively shortens the length l by the distance between surface traces, reducing the volume in the hanging wall wedge and thus reducing the forces resisting block displacement. In the case of the Chelungpu thrust, the new rupture along bedding probably has similar, if not lower, frictional resistance to the original fault, due to the flat-on-flat, bedding plane geometry of the fault. Therefore our assumption of $\mu = 0.7$ for friction is valid, and as such would not affect our calculations. The wedge now fits within the condition for the $l = 4000$ m, and our present conditions indicate that this is at equilibrium. Hence, the hinterland migration of thrusting has brought the wedge back into equilibrium.

As h increased above equilibrium values, faulting may have 'shut down' in the region until enough stress built up to overcome the static friction along bedding in the hanging wall. This hypothesis would allow the time and tectonic quiescence necessary to produce lateritic terraces. This would explain the lateritic terraces in the northern but not the southern region of the Chelungpu fault.

6. Discussion

This investigation indicates why some emergent thrust faults may have a tendency to migrate towards the hinterland.

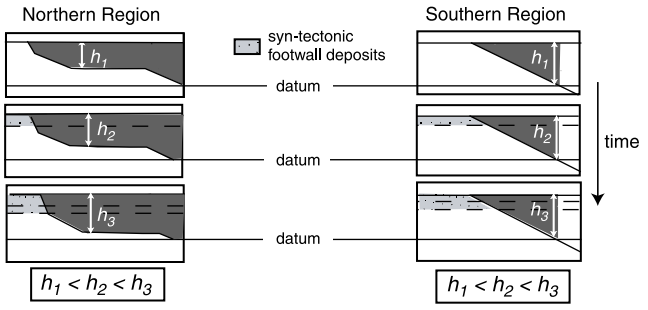

Fig. 6. Schematic model for how the hanging wall wedge thickens due to fault geometry in the near surface. Continued displacement on the fault causes footwall deposition. In response, the hanging wall must thicken as well (structural and/or 'piggy-back' deposition). The thickness of the hanging wall wedge thereby increases above the datum level where there is a flat geometry in the near surface. The thickness of the hanging wall wedge is unaffected when a planar ramp exists in the near surface (southern region). Therefore, with increasing time, the volume of the hanging wall wedge increases above the datum only where a flat exists in the near surface.

We suggest that the shape of the hanging-wall block (as dictated by original fault geometry) in the near surface determines the weight, and thus the force resisting movement during an earthquake. A shallow, footwall-flat fault geometry produces a hanging wall block in the near surface that has a much higher volume than a simple wedge above a planar fault ramp. If the resisting forces (weight of the hanging-wall in the near-surface) exceed the stress applied to the hanging wall during an earthquake, then the fault will migrate 'out-of-sequence' towards the hinterland in order to restore equilibrium. Though Yue et al. (2005) show that the structure of the Chelungpu fault is quite complex, the change from ramp to flat nevertheless occurs above 4000 m in the northern region but between 5000 and 6000 m in the southern regions. Therefore, we propose that the northern Chelungpu fault migrated from the Sanyi fault into its hanging wall due to the shallow subhorizontal detachment level in the near surface. Displacement on the Sanyi thrust during the Quaternary caused its hanging wall rocks to be tilted to the angle of the footwall ramp, as they were translated along the fault. As displacement occurred at the fault tip, continued erosion of the newly uplifted hanging wall caused the sedimentary-fill thickness in the footwall to increase. The thickness of the hanging wall block (h) (Fig. 6) increased in the northern region until a critical value was reached, where the resisting forces in the near surface ($<$ 4000 m) were greater than the tectonic load on the fault. The fault therefore could not rupture as an intact block, and thus imbricated, by stepping up or transferring slip to the higher detachment Chinsui Shale, in order to accommodate crustal shortening in this region of the fault. Similar hindward imbrication, or alternating thrusting, has been documented by Burbank et al. (1992) in the Pyrenees, Rubey et al. (1975) and Delphia and Bombolakis (1988) for the toe of the Absaroka thrust in western Wyoming, and Norris and Cooper (1997) in New Zealand. In all of these cases, the hindward imbrication occurs at the frontal part of the regional thrust system, and the imbrication occurs in regions where syntectonic conglomerates lie in the footwall. The typical spacing between the frontal and hindward thrust imbricates are 1–3 km.

Other reasons for the fault migration into the hanging wall could be the effect of the fault bend along the syncline flank. Poliakov et al. (2002) describe how a propagating rupture will naturally jump into its hanging wall as the rupture is forced around a bend. These characteristics have been observed during the Kettleman Hills earthquake (Ekstrom et al., 1992) and the Alpine fault in New Zealand (Norris and Cooper, 1997; Kent et al., 2002). The existence of optimally oriented shale bedding planes within the Kueichulin and Chinsui Shale Formations may have provided the path of least resistance for the fault rupture.

Migration of the Chelungpu fault into the hanging wall of the Sanyi Fault has produced significantly different structures between the northern and southern regions. The northern part of the Chelungpu fault is characterized by bed-parallel slip in the near surface. The fault has a narrow, 0.7–20 cm clay gouge zone to at least 250 m total vertical depth (Heermance et al., 2003). The southern part of the Chelungpu fault juxtaposes

Pliocene shale with >2000 m of Quaternary conglomerate along a footwall ramp. The fault consists of a wide (>20 m) zone of sheared clay gouge (Tanaka et al., 2002). Displacement during the 1999 earthquake was significantly less in the southern region (1–3 m) than in the northern region (5–7 m), due to the diffuse, wide fault zone (Heermance et al., 2003).

The results determined in this analysis indicate that the fault geometry in the near-surface controls surface rupture of thrust faults. For this reason, fault geometry should be considered when pre-determining potential rupture localities of faults. This simple force balance analysis can be applied to other regions where fault geometry is known, and may be utilized by the geotechnical community when considering earthquake hazards.

The region we consider here is a small toe of the tapered region considered in most 'wedge-theory' models of thrust development (Chapple, 1978; Davis et al., 1983). The region is essentially the region between the thrust wedge front and the area where the thrust slope steepens (Mouthereau et al., 2002; Fig. 1). As such, the same basic forces act, but our region is smaller that that of the entire critically tapered wedge. Thus, the imbrication mechanics here are the result of the resisting forces exceeding the tectonic load available to the wedge. The thin wedge we consider does not produce sufficient topography to be greatly influenced by the wedge geometry. Out-of-sequence thrusting at the scale of the entire thrust wedge may also be occurring (Kao and Chen, 2000), suggesting that at both the local and regional scales, the northern part of the western Taiwan thrust belt is experiencing hindward migration of active thrusting.

7. Conclusions

The southern region of the Chelungpu fault was contiguous with the Sanyi fault from between 1.0 and 0.7 Ma (W.S. Chen et al., 2001; Y.G. Chen et al., 2001). The fault ruptured along flat and ramp surfaces within late Miocene and early Pliocene sedimentary units. Some time before 46 ka, fault activity probably ceased on the Sanyi thrust in the northern region but not in the southern region. Pre-50 ka fill terraces within the lateritic terraces were formed along the river valleys and in the coastal plain. After formation of these terraces, we suggest faulting resumed along the Chelungpu/Sanyi fault segment. The fault, however, migrated back into its hanging wall in the northern region due to the shallow sub-horizontal detachment level, 55° fault dip, and wedge and block geometry. The fault did not migrate into its hanging wall in the southern region because the 25° dip and planar geometry did not require imbrication for fault emergent thrust rupture.

The mechanical model presented here shows that imbrications at the toe of a thrust complex will occur when the lower fault either encounters rocks of higher frictional resistance to slip, or if the toe lengthens, or if material is not removed from the toe fast enough. Thus, the 1–3 km hindward imbrication of thrust fronts observed in a variety of thrust belts may be a common result of this mechanical process.

Acknowledgements

Funding for this work was provided by a National Science Foundation SGER grant EAR-0098108 and a DOSECC student grant to Heermance. Discussions with S. Janecke, Z. Shipton, J.H. Hung, C.T. Lee, Y.-S. Lee, and H. Tanaka are appreciated. Reviews by D. Wiltschko and J.C. Lee are gratefully acknowledged. Thanks to J.C. Lee for finding an error in our original derivation.

References

Birkeland, P.W., 1999. Soils and Geomorphology. University Press, New York. 430pp.

Burbank, D.W., Verges, J., Munoz, J.A., Bentham, P., 1992. Coeval hindward- and forward imbricating thrusting in the south-central Pyrenees, Spain. Timing and rates of shortening and deposition. Geological Society of America Bulletin 104, 3–17.

Chang, H.C., 1994. The geological map and explanatory text of Tachia, Taiwan, Central Geologic Survey. Ministry of Economic Affairs, R.O.C., scale 1:50,000.

Chang, S.L., 1971. Subsurface geologic study of the Taichung Basin, Taiwan. Petroleum Geology of Taiwan 8, 21–45.

Chapple, W.M., 1978. Mechanics of thin-skinned fold-and-thrust belts. Geological Society of America Bulletin 89, 239–245.

Chen, C.H., Ho, H.C., Shea, K.S., Lo, W., Lin, W., Chang, H.C., Huang, C.S., Lin, C.W., Chen, G.H., Yang, C.N., Lee, Y.H., 2000. Geologic map of Taiwan. Ministry of Economic Affairs, R.O.C., scale 1:500,000.

Chen, W.S., Ridgeway, K.D., Horng, C.S., Chen, Y.G., Shea, K.S., Yeh, M.G., 2001. Stratigraphic architecture, magnetostratigraphy, and incised-valley systems of the Pliocene–Pleistocene collisional margin foreland basin of Taiwan. Geological Society of America Bulletin 113, 1249–1271.

Chen, Y.G., Chen, W.S., Lee, J.C., Lee, C.T., Chang, H.C., Lo, C.H., 2001. Surface rupture of the 1999 Chi-Chi earthquake yields insights on active tectonics of Central Taiwan. Bulletin of the Seismological Society of America 91, 977–985.

Chen, Y.G., Chen, W.S., Wang, Y., Lo, P.W., Liu, T.K., Lee, J.C., 2002. Geomorphic evidence for prior earthquakes: lessons from the 1999 Chichi earthquake in central Taiwan. Geology 30, 171–174.

Chi, W.R., Namson, J., Suppe, J., 1981. Stratigraphic record of plate interactions in the Coastal Range of Eastern Taiwan. Geological Society of China Memoir 4, 155–194.

Davis, D.J., Suppe, J., Dahlen, F.A., 1983. Mechanics of fold-and-thrust belts and accretionary wedges. Journal of Geophysical Research 88, 1153–1172.

Delphia, J.G., Bombolakis, E.G., 1988. Sequential development of a frontal ramp, imbricates, and a major fold in the Kemmerer region of the Wyoming thrust belt. Geological Society of America Special Paper 222, 207–222.

Ekstrom, G., Stein, R.S., Eaton, J.P., Eberhart-Phillips, D., 1992. Seismicity and geometry of a 110-km-long blind thrust fault 1. The 1985 Kettleman Hills, California, earthquake. Journal of Geophysical Research 97, 4843–4864.

Heermance, R.V., Shipton, Z.K., Evans, J.P., 2003. Faults structure control on fault slip and ground motion during the 1999 rupture of the Chelungpu fault. Bulletin of the Seismological Society of America 93, 1034–1051.

Ho, C.S., 1986. A synthesis of the geologic evolution of Taiwan. Tectonophysics 125, 1–16.

Ho, H.C., Chen, M.M., 2000. The geological map and explanatory text of Taichung, Taiwan. Central Geologic Survey, Ministry of Economic Affairs, R.O.C., scale 1:50,000.

Hsieh, M.L., Kneupfer, P.K., 2002. Synchroneity and morphology of Holocene river terraces in the southern Western Foothills, Taiwan: a guide to interpreting and correlating erosional river terraces across growing anticlines. Geological Society of America Special Paper 358, 55–74.

Hsieh, M.L., Lee, Y.H., Shih, T.S., Lu, S.T., Wu, W.Y., 2001. Could we have pre-located the northeastern portion of the 1999 Chi-Chi earthquake rupture using geological and geomorphic data? Terrestrial, Atmospheric and Oceanic Science 12, 461–484.

Hsieh, S.L., 1990. Fission-track dating of zircons from several east–west sections of Taiwan Island. M.S. thesis, National Taiwan University, Taipei, 134pp. (in Chinese).

Hubbert, M.K., Rubey, W.W., 1959. Role of fluid pressure in overthrust faulting. Geological Society of America Bulletin 70, 115–166.

Hung, J.H., Wiltschko, D.V., 1993. Structure and kinematics of arcuate thrust faults in the Miaoli–Cholan area of western Taiwan. Petroleum Geology of Taiwan 28, 59–96.

Hwang, R.D., Want, J.H., Huang, B.S., Chen, K.C., Huang, W.G., Chang, T.M., Chiu, H.C., Tsai, P., 2001. Estimates of stress drop of the Chi-Chi, Taiwan, earthquake of 20 September 1999 from near-field seismograms. Bulletin of the Seismological Society of America 91, 1158–1166.

Kao, H., Chen, W.-P., 2000. The Chi-Chi earthquake sequence; active, out-of-sequence thrust faulting in Taiwan. Science 288, 2346–2349.

Kent, N.W., Hickman, R.G., Dasgupta, U., 2002. Application of a ramp/flat-fault model to interpretation of the Naga thrust and possible implications for petroleum exploration along the Naga thrust front. American Association of Petroleum Geologists 86, 2023–2045.

Lee, J.C., Chen, Y.G., Sieh, K., Mueller, K., Chen, W.S., Chu, H.T., Chan, Y.C., Rubin, K.C., Yates, R., 2001. A vertical exposure of the 1999 surface rupture of the Chelungpu fault at Wufeng, western Taiwan: structural and paleoseismic implications for an active thrust fault. Bulletin of the Seismological Society of America 91, 914–929.

Lee, J.F., 2000. Geologic map and explanatory text of Tungshih, Taiwan, sheet 18. Central Geologic Survey, Ministry of Economic Affairs, R.O.C., scale 1:50,000.

Lee, Y.H., Wu, W.Y., Shih, T.S., Lu, S.T., Shieh, M.L., Cheng, H.C., 2001. Deformation characteristics of surface ruptures of the Chi-Chi earthquake, east of the Pifeng bridge. Central Geologic Survey Special Issue 12, 27–40 (in Chinese).

Lin, A., Ouchi, T., Chen, A., Maruyama, T., 2001. Co-seismic displacements, folding and shortening structures along the Chelungpu surface rupture zone occurred during the 1999 Chi-Chi (Taiwan) earthquake. Tectonophysics 330, 225–244.

Lin, C.W., Lee, Y.L., Huang, M.L., Lai, W.C., Yuan, B.D., Huang, C.Y., 2003. Characteristics of surface ruptures associated with the Chi-Chi earthquake of September 21, 1999. Engineering Geology 71, 13–30.

Liu, T.K., 1990. Neotectonic crustal movement in northeastern Taiwan inferred by radiocarbon dating of terrace deposits. Proceedings of the Geological Society of China 33, 65–84.

Lo, W., Wu, L.C., Chen, H.W., 1999. The geological map and explanatory text of Kuohsing, Taiwan. Central Geological Survey, Ministry of Economic Affairs, R.O.C., scale 1:50,000.

Meng, C.Y., 1963. The San-i overthrust. Petroleum Geology of Taiwan 2, 1–20.

Mouthereau, F., Lacombe, O., Deffontaines, B., Angelier, J., Chu, H.T., Lee, C.T., 1999. Quaternary transfer faulting and belt front deformation at Pakuashan (western Taiwan). Tectonics 18, 215–230.

Mouthereau, F., Deffontaines, B., Lacombe, O.B., Angelier, J., 2002. Variations along the strike of the Taiwan thrust belt: basement control on structural style, wedge geometry, and kinematics. Geological Society of America Special 358, 31–54.

Norris, R.J., Cooper, A.F., 1997. Erosional control on the structural evolution of a transpressional thrust complex on the Alpine fault, New Zealand. Journal of Structural Geology 19, 1323–1342.

Quin, H., 1990. Dynamic stress drop and rupture dynamics of the October 15, 1979 Imperial Valley, California, earthquake. Tectonophysics 175, 93–117.

Poliakov, A.N.B., Dmowska, R., Rice, J.R., 2002. Dynamic shear rupture interactions with fault bends and off-axis secondary faulting. Journal of Geophysical Research 107 (B11), 2295. doi:10.1029/2001JB000572. ESE 6-1 to 6-18.

Rubey, W.W., Oriel, S.S., Tracey, J.I., Jr, 1975. Geology of the Sage and Kemmerer 15′ quandrangles, Lincoln County, Wyoming, U.S. Geological Survey Professional Paper 855.

Scholz, C.H., 1998. Earthquakes and friction laws. Nature 391, 37–42.

Suppe, J., 1980. A retrodeformable cross section of Northern Taiwan. Proceedings of the Geological Society of China 23, 46–55.

Suppe, J., 1987. The active Taiwan Mountain Belt. In: Schaer, J.P., Rodgers, J. (Eds.), The Anatomy of Mountain Ranges. Princeton University Press, Princeton, New Jersey, pp. 277–293.

Tanaka, H., Wang, C.Y., Chen, W.M., Sakaguchi, S., Ujiie, K., Ito, H., Masataka, A., 2002. Initial science report of shallow drilling penetrating into the Chelungpu fault zone, Taiwan. Terrestrial, Atmospheric and Oceanic Sciences 13, 227–251.

Wang, C.Y., Huang, T.H., Yen, I.C., Wang, S.L., Cheng, W.B., 2000. Tectonic environment of the 1999 Chi-Chi earthquake in central Taiwan and its aftershock sequence. Terrestrial, Atmospheric and Oceanic Sciences 11, 661–678.

Wang, C.Y., Li, C.L., Su, F.C., Leu, M.T., Wu, M.S., Lai, S.H., Chen, C.C., 2002a. Structural mapping of the 1999 Chi-Chi earthquake fault, Taiwan by seismic reflection methods. Terrestrial, Atmospheric and Oceanic Sciences 13, 211–226.

Wang, C.Y., Tanaka, H., Chow, J., Chen, C.C., Hsueng, H.J., 2002b. Shallow reflection seismics aiding geological drilling into the Chelungpu Fault after the 1999 Chi-Chi earthquake, Taiwan. Terrestrial, Atmospheric and Oceanic Sciences 13, 153–170.

Wells, D.L., Coppersmith, K.J., 1994. New empirical relationships among magnitude, rupture length, rupture width, rupture area, and surface displacement. Bulletin of the Seismological Society of America 84, 974–1002.

Willemin, J.H., 1984. Erosion and the mechanics of shallow foreland thrusts. Journal of Structural Geology 6, 425–432.

Yu, S.B., Kuo, L.C., Hsu, Y.J., Su, H.H., Lui, C.C., Hou, C.S., Lee, J.F., Lai, T.C., Liu, C.C., Liu, C.L., Tseng, T.F., Tsai, C.S., Shin, T.C., 2001. Preseismic deformation and coseismic displacements associated with the 1999 Chi-Chi, Taiwan, earthquake. Bulletin of the Seismological Society of America 91, 995–1012.

Yue, L.-F., Suppe, J., Hung, J.-H., 2005. Structural geology of a classic thrust belt earthquake: the 1999 Chi-Chi earthquake Taiwan (Mw = 7.6). Journal of Structural Geology 27, 2058–2083.